Fuel 256 (2019) 115923

Contents lists available at ScienceDirect

Fuel

journal homepage: www.elsevier.com/locate/fuel

Full Length Article

Characterization of organosulfur compounds in asphalt cement samples by ESI(+)FT-ICR MS and ^{13}C NMR spectroscopy

Christiane F.C. Porto[a], Fernanda E. Pinto[a], Lindamara M. Souza[a], Natã C.L. Madeira[a], Álvaro C. Neto[a], Sonia M.C. de Menezes[b], Luiz S. Chinelatto Jr.[b], Carla S. Freitas[c], Boniek G. Vaz[c], Valdemar Lacerda Jr.[a,*], Wanderson Romão[a,d,*]

[a] Department of Chemistry, Federal University of Espírito Santo, Vitoria, ES, Brazil
[b] Centro de Pesquisa e Desenvolvimento Leopoldo Américo Miguez de Mello (CENPES), PETROBRAS, Rio de Janeiro, RJ, Brazil
[c] Laboratory of Chromatography and Mass Spectrometry, Institute of Chemistry, Federal University of Goiás, Goiânia, GO, Brazil
[d] Federal Institute of Education, Science and Technology of Espírito Santo, Vila Velha, ES, Brazil

GRAPHICAL ABSTRACT

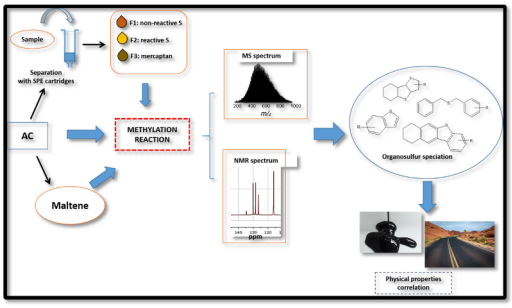

ARTICLE INFO

Keywords:
Organosulfur compounds
Asphalt cement
ESI(+)FT-ICR MS
Solid-phase extraction
^{13}C NMR
Asphalt aging

ABSTRACT

Herein, it is presented a methodology for the characterization of organosulfur compounds in asphalt cement (AC) samples employing solid-phase extraction (SPE) associated with methylation reactions and positive-ion mode electrospray Fourier transform ion cyclotron resonance mass spectrometry (ESI(+)FT-ICR MS) and carbon-13 nuclear magnetic resonance (^{13}C NMR) spectroscopy. Three AC samples were submitted to an SPE separation, and the fractions obtained the original AC samples, and their maltenes were methylated and analyzed using the ESI(+)FT-ICR MS. The ESI(+)FT-ICR MS ionized the sulfur fractions much better than the original samples, detecting organosulfur compounds with a broader average molecular mass distribution (M_w). Several types of sulfur compounds were detected, such as sulfides, disulfides, thiophenes, and dibenzothiophenes. Besides, the ESI(+)FT-ICR data were compared with the ^{13}C NMR (from model molecules analyses) and ESI(+)-Orbitrap MS. The organosulfur chemical profile was correlated to the physical properties of AC samples. It was verified that the samples with higher aromatic-character were less susceptible to aging test, while the one with more saturated-character presented more significant variation in their physical properties after the aging test.

* Corresponding authors at: Department of Chemistry, Federal University of Espírito Santo, Vitoria, ES, Brazil (W. Romão).
E-mail address: wanderson.romao@ifes.edu.br (W. Romão).

https://doi.org/10.1016/j.fuel.2019.115923
Received 24 April 2019; Received in revised form 26 July 2019; Accepted 29 July 2019
Available online 13 August 2019
0016-2361/

1. Introduction

Asphalt cement (AC) is composed of the heavier fraction from petroleum distillation, which is the vacuum residuum [1]. AC is widely used as pavement asphalt binder because it has favorable characteristics such as flexibility and adhesion [2]. The AC is a matrix of great chemical complexity, and its composition will depend on the original oil, the refining process that was used, and to oxidation reactions suffered in the machining processes [4].

The chemical composition of asphalts is essential for the understanding of the aging processes and oxidation mechanisms that cause degradation over the lifetime of the pavement [3,5]. Oxidative processes can cause changes in the physicochemical and rheological properties, which consequently will interfere with the quality and durability of the asphalt [6,7].

Sulfur is the most abundant heteroatomic compounds class in petroleum and its derivatives [7]. The presence of these compounds in high concentration in AC is closely related to the aging processes because oxidation affects their chemical composition [7,8]. According to the literature, sulfur is found in the asphaltic binder primarily in the form of thiophenes and their derivatives (benzo and dibenzothiophenes), sulfides, and sulfoxides [4,9,10]. According to Mill [11], aliphatic sulfides are more reactive to the attack of oxygen in the aging process, being oxidized to sulfoxide with mechanisms involving hydroperoxides, while the thiophene groups are more resistant to oxidation. Sarret et al. [9] verified that the sulfur-containing compounds' speciation is directly related to the oxidation state of asphalts, i.e., the types of sulfurated compounds present in the binder can indicate the aging stage. Carvalho et al. [4] conducted a study of the sulfur distribution in acidic, basic, and neutral fractions present in maltene fraction and asphaltic binder asphaltenes, before and after aging tests. They observed that the transformation of the neutral sulfur compounds, i.e., less reactive, into resins might be related to ring breaking reactions of thiophene compounds [4]. Thus, the speciation of the polar compounds in the asphalt binder can be used to gauge the quality of the asphalt, primarily regarding the understanding of the aging process, as well as the development of more resistant asphalts [4].

Several techniques have been applied in the determination of organosulfur compounds in AC, such as gas chromatography and liquid chromatography [12–14] and two-dimensional gas chromatography [13,15]. However, the high complexity of the asphalt matrix is an interfering factor that reduces the ability of these techniques to characterize all components of interest fully [16–19].

Ultrahigh-resolution mass spectrometry has been reported as one of the most efficient and complete techniques in the petroleomics area, which can be achieved by equipment such as the Fourier transform ion cyclotron resonance mass spectrometer (FT-ICR MS) [20–27] and Orbitrap [16,28]. To detect organosulfur compounds in a complex mixture, firstly, they must be effectively ionized as molecule-ions. For this, several soft ionization techniques, such as electrospray ionization (ESI) [20–26], atmospheric pressure photoionization (APPI) [29,30], and atmospheric pressure chemical ionization (APCI) [31], can be utilized, making possible a determining the composition of a wide range of organic chemical species. It is crucial to notice that it is difficult to use a unique ionization technique to completely ionize all the sulfur compounds present in the crude oil matrix due to the limitations of each technique. [13,32] Among the ionization techniques, ESI and APPI are the most used for the analysis of organosulfur petroleum derivatives. Both techniques are capable of to ionize several types of sulfur compounds such as thiols, sulfides, polysulfides and thiophenes, and in general, polycyclic aromatic sulfur heterocycles (PASHs). However, to be analyzed by ESI, it is necessary to apply derivatization techniques, but for APPI, they are not necessary [13,29].

Electrospray ionization (ESI) is one of the most common ionization techniques applied for polar compounds' characterization (heteroatom compounds) in petroleum and its products [13,20–26]. Routinely, these polar compounds are identified in positive ionization mode if they are basic [21,33] or in negative mode if they are acids [23]. The sulfur compounds are not sufficiently acidic or basic to be detected directly by ESI. Therefore, a chemical derivatization reaction is needed to pre-ionize those compounds [20–22,34–37]. Among them, the methylation reaction has been used to convert the sulfur compounds in highly polar methyl sulfonium salts allowing the analysis in the positive ionization mode (ESI(+)) [22,34–37]. The methylation reaction is a bimolecular nucleophilic substitution (S_N2) where sulfur (nucleophile) reacts with the iodomethane (alkyl halide) in the presence of silver tetrafluoroborate(III) ($AgBF_4$) forming sulfonium salts, which are stabilized by the BF_4^- anion, as shown in Fig. 1. Iodine (halogen substituent) is captured by Ag^+ forming a silver iodide precipitate (AgI) [38,39].

The efficiency of ESI(+) ionization of sulfur compounds can be further improved by the use of solid-phase extraction (SPE). SPE can decrease the matrix effect [40] and enable the detection of a greater range of sulfur compounds (reactive compounds (sulfides and disulfides) and nonreactive (thiophenes)) [41].

The SPE method has been widely applied for fractionation of petroleum and its derivatives due to its simplicity, rapid preparation, low solvent volume, and fast sample recovery [7,16,49,42]. Vasconcelos et al. [16], used SPE to extract nitrogen compounds in vacuum residues. Silveira et al. [7] employed a cleaning method using SPE for the organosulfur determination in AC samples. Lobodin et al. [41] applied SPE to separate reactive sulfur compounds (sulfides and disulfides) and nonreactive (thiophenes) of various petroleum cuts, showing that the use of the SPE extends the characterization by ESI(+)FT-ICR MS of sulfur species in petroleum.

Thus, in this study, the organosulfur compounds present in three samples of AC and their respective fractions of maltenes were methylated. Samples were characterized using ESI(+)FT-ICR MS, ESI(+)Q-Exactive Orbitrap MS and ^{13}C NMR spectroscopy. The last technique was also used in a study of 10 model sulfur compounds. Subsequently, the SPE method was used to produce three different sulfur fractions (reactive, nonreactive, and mercaptan) from AC samples. The fractions produced were methylated and characterized using ESI(+)FT-ICR MS. The results obtained before and after the SPE separation method were compared, and some correlations were proposed in the function of the physical properties of AC samples.

2. Materials and methods

2.1. Reagents and materials

The reagents used in the methylation reaction were iodomethane (99% CH_3I), iodomethane enriched with ^{13}C (99% ^{13}C, $^{13}CH_3I$), silver tetrafluoroborate(III) (98% $AgBF_4$), anhydrous 1,2-dichloroethane (99.8% $C_2H_4Cl_2$), all being purchased from Sigma Aldrich (St. Louis, USA). The *n*-hexane solvent (95% C_6H_{14}) was supplied by Tedia (Rio de Janeiro, BR). The model sulfur compounds studied by ^{13}C NMR were:

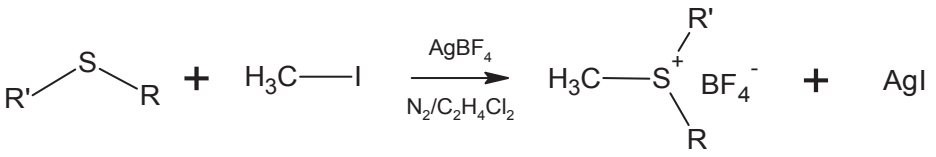

Fig. 1. A general example of a typical methylation reaction.

dibenzothiophene (98% $C_{12}H_8S$), naphtho[1,2-*b*:5,6-*b*′]dithiophene (97%, $C_{14}H_8S_2$), 1-propanethiol (99% C_3H_7SH), 2-naphthalenethiol (99% $C_{10}H_7SH$), 3-methylbenzothiophene (96% C_9H_8S), 4,6-diethyldibenzothiophene (97% $C_{16}H_{16}S$), diphenyl sulfide (98% $(C_6H_5)_2S$), diisopropyl sulfide (99% $[(CH_3)_2CH]_2S$), tetrahydrothiophene (99% C_4H_8S), and thianaphthene (98% C_8H_6S). The reagents used in the NMR analysis were chloroform-*d* (99.8% D, $CDCl_3$), acetonitrile-d_3 (99.96% D, CD_3CN), and chromium(III) acetylacetonate (97% $Cr(acac)_3$), being purchased from Sigma Aldrich (St. Louis, USA). For the ES(+)FT-ICR MS analysis, methanol (CH_3OH 99.9%) and formic acid (99% CH_2O_2) were obtained from Sigma Aldrich (St. Louis, USA) and toluene (C_7H_8 98%) from Vetec (Rio de Janeiro, BR). For the extraction procedure, dichloromethane (DCM, 99.5% CH_2Cl_2) was purchased from Exodus Scientist (São Paulo, BR). Acetone (ACE, 99.5% C_3H_6O) and hydrochloric acid (HCl, 37% HCl) were obtained from Proquimios (Rio de Janeiro, BR). Acetonitrile (ACN, 99.5% CH_3CN) and methanol (MeOH, 99.8% CH_3OH) from Dinâmica (São Paulo, BR), toluene (TOL, 99.9% C_7H_8) and silver nitrate ($AgNO_3$, < 100%) from Sigma Aldrich (St. Louis, USA). All reagents were used as received. The SPE cartridges (Strata® SCX) filled with 2 g benzene sulfonic acid bound silica were purchased from Phenomenex (CA, USA).

2.2. Samples

AC samples were provided by PETROBRAS (Rio de Janeiro, Brazil) and named AC 1, AC 2, and AC 3. Their respective physicochemical properties are summarized in Table 1. All tests were conducted by the PETROBRAS Research and Development Center (Centro de Pesquisas Leopoldo Américo Miguez de Mello-CENPES, Rio de Janeiro, Brazil). The content analysis of asphaltenes, aromatics, and resins were obtained by determining saturated, aromatics, resins, and asphaltenes (SARA) using the supercritical fluid chromatography with flame ionization detection (SFC-FID) technique [43]. Total nitrogen was determined according to the UOP 384-76 standard by acid extraction or direct Kjeldahl procedure [44]. Total basic nitrogen and the weak acidity were determined by potentiometric titration according to the UOP 269-90 and ASTM D664 standards, respectively [45,46]. Total sulfur was determined according to ASTM D1552, by infrared and high combustion temperature or by thermal conductivity [47]. Physical tests were performed by AC samples such as retained penetration (ASTM D5), softening point (ASTM D36), and capillary viscosity (ASTM D2171, Rolling Thin-Film Oven Test, RTFOT, and ASTM D2872) [48–51].

2.3. Maltene fraction extraction

The maltene fraction extraction of the AC samples was realized by the precipitation of asphaltenes, according to the ASTM D6560-00 norm [52]. However, to promote better precipitation of asphaltenes, *n*-pentane was used instead of *n*-heptane, as described in the literature [52]. It was also chosen to study the fraction of maltenes because a significant part of the resins and asphaltenes were preferentially precipitated.

Table 1
Physicochemical properties of AC samples.

Properties	AC 1	AC 2	AC 3
Total nitrogen (wt%)	0.57	0.43	0.96
Total basic nitrogen (mg/kg)	2296	1137	3178
Total sulfur (wt%)	0.64	5.02	0.90
Weak acidity (mg KOH/g)	1.19	< 0.10	1.02
Asphaltenes (wt%)	34	20	19
Aromatics (wt%)	38	47	45
Resins (wt%)	20	28	28
Retained penetration	0.67	0.63	0.67
Softening point increasing (°C)	5.8	4.1	4.6
Capillary viscosity ratio	3.12	1.93	2.35
RTFOT – mass balance (%)	(+) 0.027	(+) 0.0192	(−) 0.1259

2.4. Solid-phase extraction

The extraction of the sulfur fractions was performed as described by Lobodin et al. [41]. The extraction procedure, shown in Fig. 1S is divided into two steps: modification of the stationary phase and extraction of the sulfur fractions. The sample mass fractionation contained 5 mg of sulfur. Because of the high viscosity of the samples, they were previously diluted in 2 mL of DCM. The extraction procedure was applied to the three AC samples generating a set of nine fractions, three fractions for each AC.

2.5. Methylation reaction

The methylation reactions of the sulfur compounds were conducted according to Jaramillo et al. [39] with some modifications to improve the methylation efficiency of AC. The methylation reactions were performed on the AC and maltenes samples as well as in the fractions separated by SPE extraction. Briefly, a mass sample containing 0.65 mmol of sulfur was dissolved in approximately 5.0 mL of $C_2H_4Cl_2$. Under stirring and nitrogen atmosphere, 1.5 mmol of CH_3I in the form of a 1% solution in dichloroethane (w/v) was added dropwise over approximately 1 h. A solution of 1.3 mmol of $AgBF_4$ in 3.0 mL of dichloroethane was slowly added. The reaction was allowed to occur for 48 h under stirring and nitrogen atmosphere. Centrifugation removed the silver iodide (AgI) precipitate formed in the reaction. The supernatant liquid was separated, and a rotary evaporator removed the solvent. The product obtained was washed with five portions of *n*-hexane to remove the unreacted compounds and left in the flask until completely dry. The methylated samples were named as follows: AC 1-M, AC 2-M, and AC 3-M (methylated ACs); MALTENE AC 1-M, MALTENE AC 2-M, and MALTENE AC 3-M (methylated maltenes); and F1-M, F2-M, and F3-M (methylated fractions).

2.6. ESI(+)FT-ICR MS and ESI(+) Q-Exactive Orbitrap MS analyses

ESI(+)FT-ICR MS analyses were performed on a 9.4 T FT-ICR mass spectrometer (Solarix, Bruker Daltonics, Bremen, Germany) operating at an ion acquisition range of *m/z* 200–2000 and data were acquired at a resolution power of 450,000 at *m/z* 400. Samples were diluted with toluene:methanol solution (50:50 v/v) at a concentration of 1 mg mL^{-1}, added of 0.1% formic acid. The resultant solution was directly infused into the ESI source at a flow rate of 20 μL min^{-1}. The ESI(+) source conditions were as follows: nebulizer gas pressure at 2.0 bar, the capillary voltage at 2.8 kV, and ion transfer temperature of 180 °C. Ion accumulation time and time of flight (TOF) in the hexapole were 0.20 s and 1.0 ms, respectively. Each spectrum was acquired with an accumulation of 200 scans of transient signals in the 4 M time-domain (mega point). The equipment was externally calibrated from an arginine solution at a concentration of 0.05 mg mL^{-1} [35].

The ESI(+) Q-Exactive Orbitrap analyses were performed on the *Q-Exactive™ Hybrid Quadrupole-Orbitrap* spectrometer (Thermo Scientific, Bremen, Germany). The sample preparation procedure was similar to that used for the ESI(+)FT-ICR MS analysis. The resultant solution was directly infused at a flow rate of 5 μL min^{-1}. The analysis conditions were as follows: sheath gas and auxiliary of 20 and 0 bar, respectively; a capillary temperature of 275 °C; capillary voltage of 4.0 kV; and S-lens of 50%. Each spectrum was acquired with an accumulation of 50 scan events in full MS mode. Mass range was set to *m/z* 200–1200, and data were acquired at a resolution setting of 140,000 at *m/z* 200 at full profile format [16].

The obtained mass spectra acquired by ESI(+)FT-ICR MS and Q-Exactive were processed by the Composer® (Sierra Analytics, Pasadena, CA, USA) and Xcalibur 2.2 (Thermo Fisher Scientific) software. For better visualization and interpretation of the data, graphs of the relative distribution of the classes, the relative distribution of the classes as a function of the double bond equivalent (DBE) and DBE as a function of

the carbon number (CN) were plotted.

2.7. NMR analysis

^{13}C NMR analyses were performed on a Varian 400 MHz spectrometer using 5.0 mm BroadBand ^{1}H/^{19}F/X probe at 26 °C. 100 mg of each sample was dissolved in 600 µL of a mixture of acetonitrile-d_3 and chloroform-d (1:2 v/v), with the addition of relaxation agent (Cr(acac)$_3$) at a concentration of 0.05 mol L^{-1}. For the model sulfur compounds, 20 mg of each sample was dissolved in 600 µL of a mixture of acetonitrile-d_3 and chloroform-d (1:2 v/v), without the addition of relaxation agent. The nuclear Overhauser enhancement was suppressed by operating the spectrometer in the "inverse-gating" mode, where the broadband proton decoupling was turned on only during acquisition periods. Data analysis was performed using MestreNova software, applying to phase correction, and baseline correction manually. The parameters used in the analyses are described in Table 1S.

3. Results and discussion

3.1. ESI(+)FT-ICR MS

3.1.1. Asphalt cements and maltenes

Figs. 2 and 3 show ESI(+)FT-ICR mass spectra from ACs and their maltene fractions, respectively, before and after the methylation reaction. For the nonmethylated AC, Fig. 2, the average molecular weight distribution values (M_w) varied by 87 Da (M_w = 664–751 Da), while for the methylated AC samples, Fig. 3, this variation was only by 23 Da (M_w = 710–733 Da). This minor variation of M_w observed among the methylated AC is due to the methylation reaction, which favors the selective ionization of the sulfur derivatives compounds class. After this process, the AC 1–3 M samples (Fig. 2d–f) presented a more efficient ionization, increasing the signal-to-noise ratio, and consequently, the amplitude of organosulfur compounds detected (from m/z 300 to 1100). This behavior is primarily demonstrated for the AC 2-M sample, which is rich in total sulfur (5 wt%, Table 1), causing the greater M_w variation observed among AC 2 and AC 2-M samples (46 Da, 664 → 710 Da, Fig. 2b and e, respectively). Thus, after being subjected to the methylation reaction, the sulfur compounds acquire a positive charge and decrease the ionic suppression effect caused by compounds that have smaller values of pK_b (pyridine compounds and their analogs) [16].

Comparing the ESI(+)FT-ICR mass spectra of the maltenes samples (Fig. 3a–f), the methylation reaction can increase the M_w values for all samples (from 657 to 705 Da, Fig. 3a–c, to 710–754 Da, Fig. 3d–f). The increase of M_w values between the methylated samples (which obeys the following order: MALTENE AC 1-M (710 Da) < MALTENE AC 3-M (723 Da) < MALTENE AC 2-M (754 Da)), corroborates with the total S content detected as shown in Table 1 (total S: 0.64 < 0.90 < 5.02 wt %, respectively). It is important to emphasize that in the maltenes, the aromatic compounds are concentrated because the majority of resins and asphaltenes were precipitated in the extraction process of the same ones [53]. Therefore, for being a less complex fraction than the original AC, probably, the methylation reaction occurs more easily in this matrix due to the greater mobility of the compounds in solution, favoring the contact between the sulfur compounds and the derivatizing agent. Hence, a larger amount of sulfur compounds with higher M_w values are identified. According to the results of AC 2 (Fig. 3b), after the methylation, a shift of the Gaussian profile was observed, increasing the M_w values from 657 to 754 Da (Fig. 3b and e).

The relative distribution of heteroatomic classes detected in ACs and maltenes are illustrated in Fig. 4a–d. AC and maltene samples before methylation (Fig. 4a and c, respectively) present the N_1[H], O_3[H], and N_2[H] classes in greater abundance. After methylation, sulfur classes were mostly detected, highlighting in the AC samples (Fig. 4b) the following classes: NS[H] and S_2[H] for AC 1-M, S_1[H] and S_2[H] for AC 2-M, and S_1[H] for AC 3-M. For the maltenes (Fig. 4d), the classes found are S_1[H] for MALTENE AC 1-M, S_1[H] and S_2[H] for MALTENE AC 2-M, and S_1[H] for MALTENE AC 3-M. AC 2 and MALTENE AC 2 samples, after methylation, present a greater abundance of the S_1[H] class in comparison with the other samples, corroborating with the data described in Table 1.

Fig. 2sa–d shows the relative distribution of S_1[H] and S_2[H] classes as a function of DBEs for methylated ACs and maltenes samples. For AC 2-M sample and its respective maltene fraction, the S_1[H] class (Fig. 2Sa and Sc) had a higher DBE distribution (2–17), with the global maximum at DBE = 6–7. The other samples had less intensity for this class and DBE distribution ranging from 1 to 14, FFig. 2Sa and Sc, except for the AC 1-M sample (Fig. 2Sa), where the presence of the S_1[H] class was not detected.

The S_2[H] class (Fig. 2Sb–d) was detected in the AC 1-M, AC 2-M (Fig. 2Sb), and MALTENE AC 2-M (Fig. 2Sd) samples. The DBE distribution for the AC 2-M and their respective maltene fraction, is identical, ranging from 8 to 18 with the global maximum at DBE = 12. Therefore, a greater abundance of sulfur compounds with a higher aromatic character was detected, i.e., derivatives of benzo and dibenzothiophenes. For the AC 1-M sample (Fig. 2Sb), compounds of higher aliphatic nature with DBE distribution from 0 to 10 was detected, with maximum abundance at DBE = 0–2, indicating the presence of saturated aliphatic disulfides (DBE = 0), and disulfides in naphthenic structures with 1–2 rings (DBE = 1–2). In the AC 1 sample, a difference in the chemical profile of the sulfur compounds was

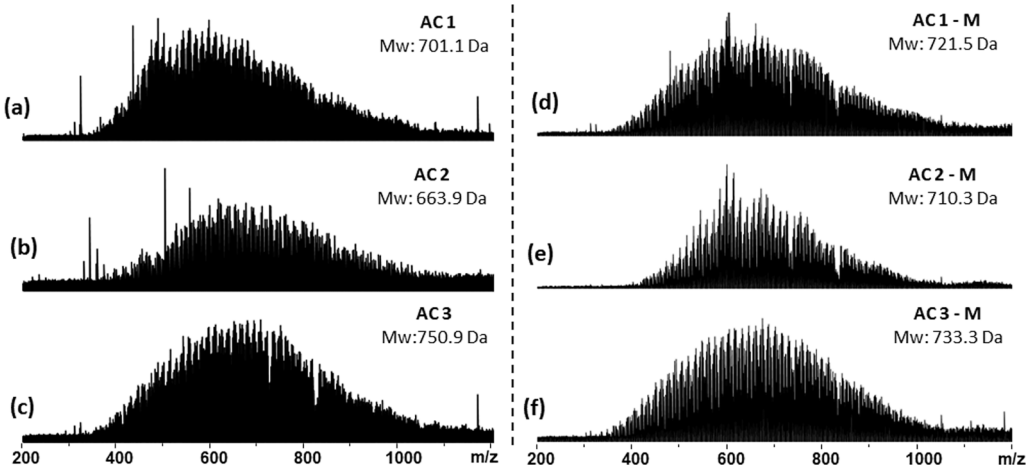

Fig. 2. ESI(+)FT-ICR mass spectra of the ACs before (a–c); and after the methylation reaction (d–f).

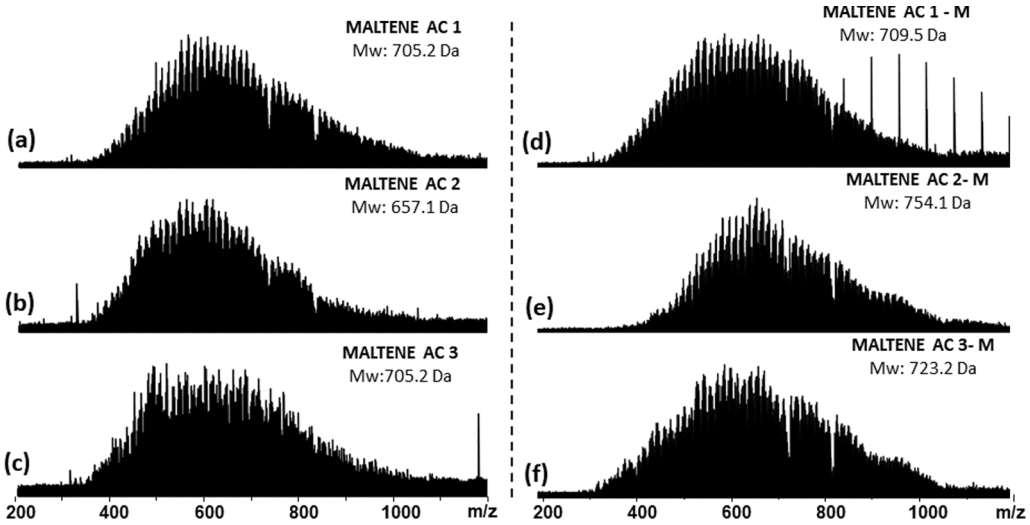

Fig. 3. ESI(+)FT-ICR mass spectrum of the maltenes before (a–c), and after the methylation reaction (d–f).

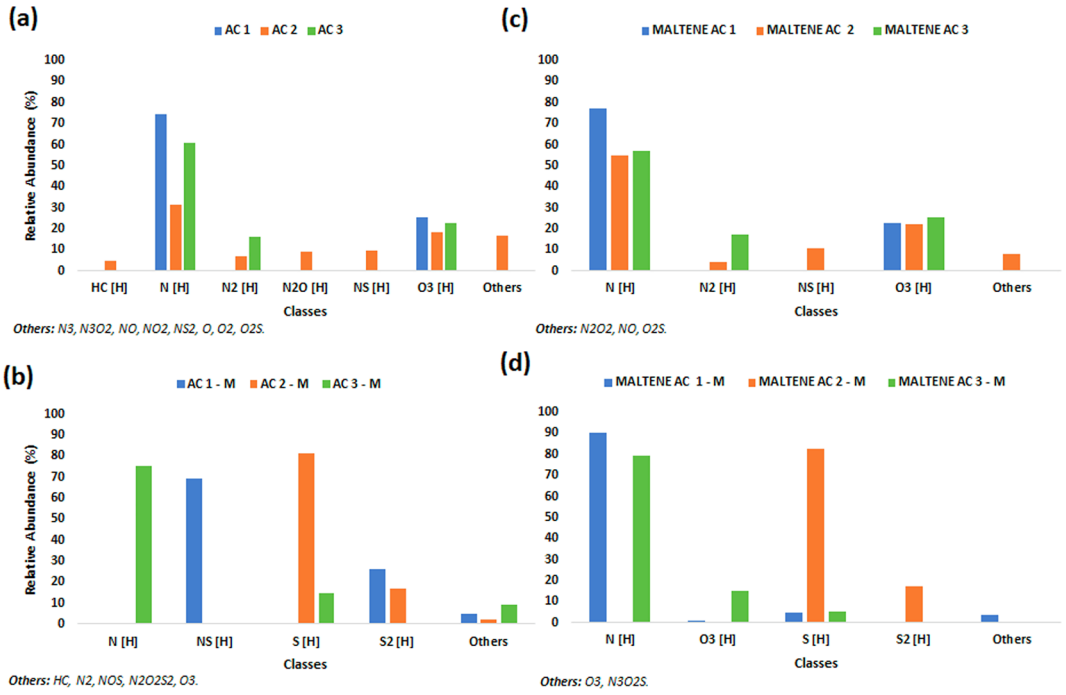

Fig. 4. Relative distribution of heteroatomic classes of ACs and maltenes before (a, c); and after methylation reaction (b, d).

detected. This sample differs from others regarding SARA content. Thus, for the AC 1 sample, it can be inferred that the distribution of the sulfur compounds differs between the fractions of aromatics (maltenes), asphaltenes, and resins (asphalt cement).

The DBE plots as a function of CN of the methylated AC samples are shown in Fig. 5a–i for S_1[H] (5a, d, g), S_2[H] (5b, e, h), and NS[H] (5c, f, i) classes. In the AC 1-M sample, the S_2[H] class (Fig. 5b) showed a distribution of compounds with DBE ranging from 0 to 12 a CN from C_{26} to C_{70} with a maximum abundance at DBE = 0 and CN of C_{40}, deriving from saturated aliphatic chain disulfides. For the NS[H] class (Fig. 5c), the compounds detected had a DBE distribution from 0 to 19 and CN from C_{25} to C_{82} with a global maximum at DBE = 7 and CN of C_{45}. These species correspond to saturated and aromatic condensed rings containing N and S atoms in their structure, such as pyridine and thiophenes derivatives [32]. The S_1[H] class (Fig. 5a) was not detected in the AC 1 sample. Concerning the AC 2 sample (Fig. 5d–f), the S_1[H] class (Fig. 5d) showed the distribution of compounds of DBE from 1 to 18 and CN from C_{29} to C_{72} with a global maximum at DBE = 7 and CN of C_{60}, which corresponds to a benzothiophene with saturated ring aggregate. The S_2[H] class (Fig. 5e) showed a DBE distribution ranging from 7 to 19 with CN from C_{31} to C_{66}, with greater intensity in species of DBE = 12 and CN of C_{50}, derived from benzothiophenes condensed with saturated ring aggregated in its structure [54]. In AC 3, the S_1[H] class (Fig. 5g) presented a DBE range from 1 to 15 and CN from C_{29} to C_{67}, with greater intensity in DBE = 6 and CN of C_{43}, which is attributed to benzothiophenes [54]. Comparing the species population detected in the three samples, concerning the S_1[H] class, AC 2-M and AC 3-M samples presented similar aromaticity, basically consisting of thiophene compounds. However, in the AC 2-M sample, these species concentrated a higher value of CN (C_{60}). Thus, AC 2-M sample has thiophene compounds of greater value of M_w than sample AC 3-M. For the S_2[H] class, the species found in the AC 1-M and AC 2-M samples had distinct characteristics. For the AC 1-M sample, the most intense species were disulfides of saturated aliphatic character. Conversely, the

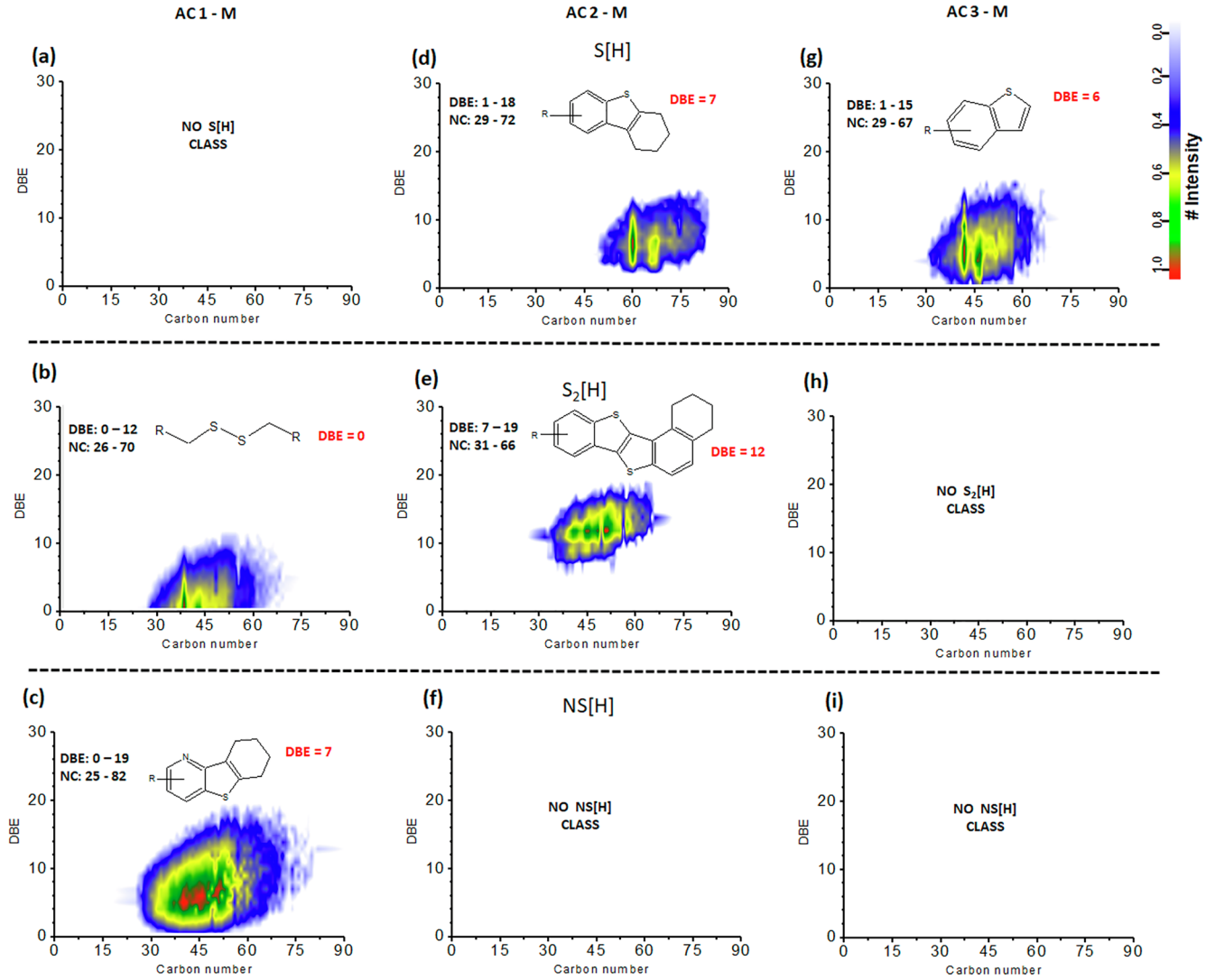

Fig. 5. DBE as a function of carbon number for S_1[H], S_2[H], and NS[H] classes of AC 1-M (a–c); AC 2-M (d–f), and 3-M AC (g–i) samples. Proposed sulfur compounds are represented for DBEs indicated in red. (For interpretation of the references to colour in this figure legend, the reader is referred to the web version of this article.)

AC 2-M sample had a higher concentration of high aromaticity species, such as derivatives of condensed benzothiophenes. As expected, sulfur compounds detected with higher intensity in the samples were sulfides, thiophenes, and dibenzothiophenes, species typically found in petroleum products [4,9,10,41].

3.1.2. Sulfur fractions

The sulfur separation procedure was applied only to AC, and three fractions were extracted: F1, F2, and F3. The F1 fraction is composed of stable sulfur species such as thiophenes and dibenzothiophenes (where sulfur is part of the aromatic system) and diaryl sulfides (where sulfur is directly attached to the aromatic ring) such as diphenyl sulfides and their homologs. The F2 fraction is composed of thiols, sulfides, and F3 fraction corresponds to mercaptans, which were recovered at the end of the process by a hydrochloric acid and methanol mixture, followed by other solvents [41]. The F1 sample is extracted by ACE:DCM addition, while F2 by ACN:DCM addition. The ACE:DCM mixture is less polar than ACN:DCM. Thus, the F1 fraction will contain more aromatic compounds, which are less polar than the sulfides species that compose the F2 fraction. The mercaptans react with the Ag^+ of the stationary phase, forming insoluble salts that are retained in the SPE cartridge. Therefore, it is necessary to add the HCl:MeOH mixture, to solubilize these salts, allowing the extraction of mercaptans [41]. The mass balance was performed, and recovery percentages for each fraction produced are shown in Table 2S. As can be noted, the highest percentage of the recovery sample was observed for the AC 2 sample, indicating that it has a higher sulfur content, whereas the sample AC 1 presents the lowest percentage of the recovery. These results corroborate with the sulfur percentage (in wt%) reported in Table 1.

Fig. 6a–f shows the ESI(+)FT-ICR mass spectra of the F1, F2, and F3 fractions, from the AC that has a higher total sulfur content, i.e., the AC 2 sample, and the class distribution graphs are shown in Fig. 6(g, h). The F1 (Fig. 6a) and F2 (Fig. 6b) fractions were only ionized after the methylation reaction (Fig. 6d and e, respectively) because these fractions had a higher abundance of sulfur compounds. However, the F3 fraction (Fig. 6c) is composed not only of mercaptan species, nitrogenous and oxygenated species being detected before methylation. The methylated fractions showed a Gaussian profile with *m/z* range of 200–1200, and M_w centered at 824.8 Da for F1-M, 725.5 Da for F2-M, and 705.1 Da for F3-M. Similar behavior was observed for ESI(+)FT-ICR mass spectra for F1–F3 fractions of the AC 1 and AC 3 samples (Figs. 3S and 4S).

Comparing the M_w values of the methylated AC 2 fractions (Fig. 6) with its original methylated sample (Fig. 2e), a wider distribution of compounds ranging from *m/z* 200 to 1200 was observed for Fig. 6d–f, which for the original methylated sample (Fig. 2e), this range varied

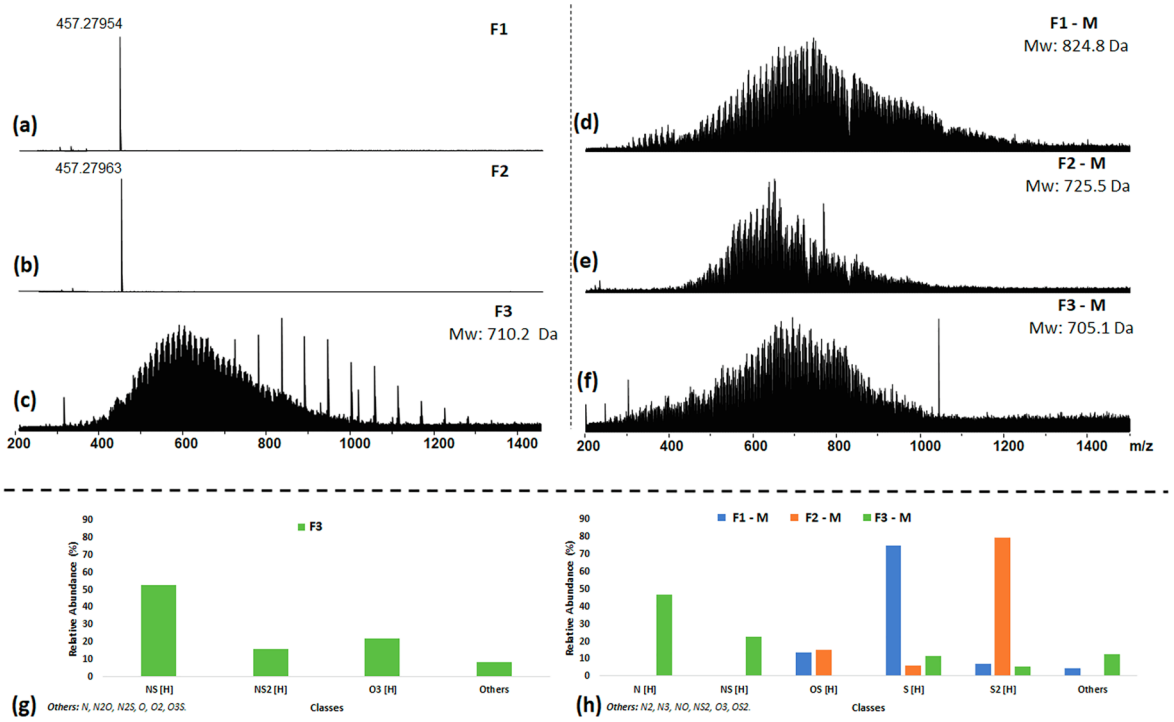

Fig. 6. ESI(+)FT-ICR mass spectra of the AC 2 fractions, (a–c) before methylation and (d, e) after methylation. The class distribution graph is displayed in Fig. 6g, h for the fractions (g) before and (h) after the methylation reaction.

from *m/z* 300 to 1100. Therefore, this result indicates a better ionization efficiency of sulfur compounds when the fractionation process is applied. From the fractionation method, for sample AC 2, 1909, 1060, and 3408 were assigned in the samples F1-M, F2-M, and F3-M, respectively, totaling 6377 compounds detected, while in the non-fractionated sample (Fig. 2e), 971 compounds were only identified. Selective extraction reduced the ionic suppression effect, caused by species of lower M_w values, as well as species of lower pK_b values, that can ionize more quickly than typical sulfur compounds. Another great advantage of this methodology is the decrease of matrix complexity over the compounds of interest [16].

Figs. 6h, and 5S shows the class distribution diagram for AC 2, AC 1/AC 3 samples, respectively. Fig. 6h shows that five classes of sulfur compounds were detected after selective fractionation (S[H], S_2[H], NS[H], NS_2[H], and OS[H] classes). Conversely, for the F3 fraction without methylation reaction and the AC 2-M sample (Fig. 4b) only two (NS[H] and NS_2[H]) and three (S_1[H], S_2[H], and $N_2O_2S_2$[H]) classes of sulfur compounds were detected, respectively. Therefore, this confirms the higher selectivity of the fractionation method for detecting sulfur compounds' derivatives. The proportions of S_1[H] and S_2[H] classes found for the F1-M and F2-M samples corroborate with the results obtained by Lobodin et al. [41], which characterized the presence of reactive and nonreactive sulfur compounds in vacuum gas oil samples.

The relative distribution of sulfur classes as a function of the DBE is shown in Figs. 7, and 6S for the fractions of AC 2, and ACs 1 and 3 samples, respectively. In Fig. 7a, the DBE range of S_1[H] and S_2[H] classes of the F1-M sample has compounds with maximum DBE abundance more significant than that observed for F2-M (Fig. 7b). This behavior agrees with the extraction methodology applied because the F1-M fraction is composed of species with higher aromatic character than the F2-M fraction. In Fig. 7a, b, for F1-M and F2-M samples, the most abundant sulfur classes were S_1[H], S_2[H], and OS[H] classes. The OS[H] class presented a higher amplitude of DBE distribution (1–14) for the F1-M sample (Fig. 7a). For the F3-M sample, the DBE range of the detected classes (Fig. 7c) is higher. Theoretically, for this fraction, low values of DBEs were expected because F3-M is composed of mercaptans [13]. However, besides the sulfur class (Fig. 6g, h), other classes were extracted, such as oxygenated and nitrogenated classes. The most abundant sulfur class of F3-M was NS[H] (Fig. 7c), with DBE ranging from 2 to 26, thus, is the most aromatic class among all the sulfur classes detected.

The DBE distribution graph for the S_1[H] and S_2[H] classes as a function of the CNs for the methylated fractions of the AC 2 are presented in Figs. 8a–f, and 7S for fractions of the AC 1 and AC 3 samples. In the F1-M fraction, the class S_1[H] (Fig. 8a) presented DBE distribution ranging from 5 to 20, with higher intensity in DBE = 10, and CN at C_{50}, corresponding to dibenzothiophene derivatives with one aggregate saturated ring. The S_2[H] class (Fig. 8b) showed DBE ranging from 9 to 21, with higher abundance in DBE 15 and CN at C_{47}, which is attributed to benzothiophenes structure fused to one saturated ring and one aggregated aromatic ring [13]. In the F2-M fraction, the S_1[H] class (Fig. 8c) presented DBE distribution ranging from 3 to 16, with higher intensity in DBE 7 and CN at C_{45}, which corresponds to the benzyl sulfides with three saturated rings or to sulfides, where sulfur within a saturated ring is attached to naphthenic and/or aromatic rings. The S_2[H] class (Fig. 8d) showed DBE distribution ranging from 8 to 19, with maximum distribution in DBE 12 and CN at C_{50}, which corresponds to disulfides, where sulfur atoms are connected on a system of three aromatic rings with one aggregated saturated ring. Another possibility is a structure where sulfur atoms are within the saturated rings attached to other saturated and aromatic rings [41,54].

In the F3-M sample, the S_1[H] class (Fig. 8e) presented DBE distribution varying from 3 to 17, with the maximum centered at DBE 6 and CN of C_{45}, corresponding to benzothiophene structure. The S_2[H] class (Fig. 8f) presents DBE distribution varying from 5 to 19, with more significant intensity at DBE 11 and CN at C_{57}, consisting of condensed benzothiophene structure [41]. These results demonstrated that mercaptans were not present in this sample or they were not extracted in the extraction procedure, but instead, species containing a higher aromaticity degree, as previously observed.

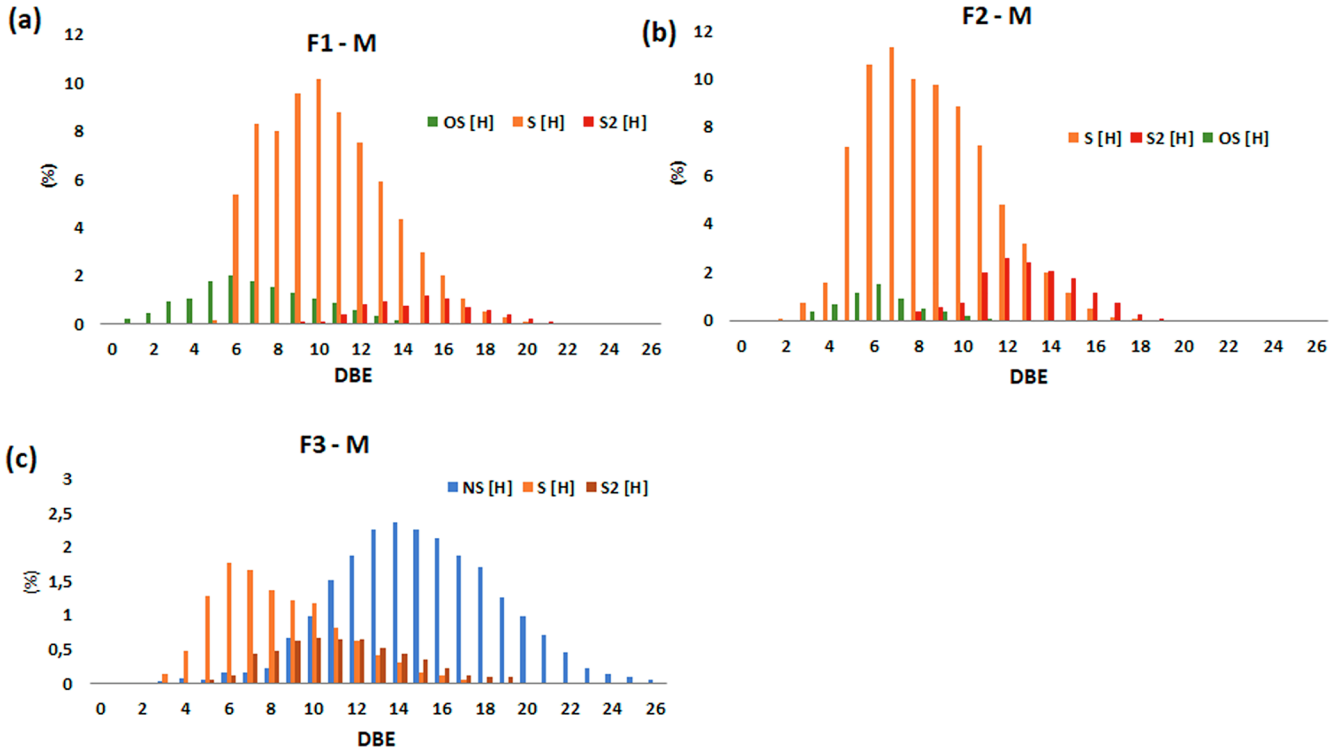

Fig. 7. Relative distribution of DBE for the sulfur classes in (a) F1-M, (b) F2-M, and (c) F3-M fractions of the AC 2 sample.

3.2. ^{13}C NMR

Fig. 9 shows a comparison between the ^{13}C NMR spectrum of AC 2, before and after methylation. The methylation reaction for the ^{13}C NMR analyses was performed according to the methodology described for the ESI(+) analyses, but now containing the isotopically enriched iodomethane with ^{13}C (99% ^{13}C). The purpose of using this reagent is to increase the detection sensitivity to the ^{13}C nucleus of the methyl that was added in the reaction. Thus, after methylation, the signals of the methyl groups will stand out relative to the signals of the other components in the sample, which are in higher number. The chemical shift values (δ) of the ^{13}C methyl group observed in the ^{13}C NMR spectrum

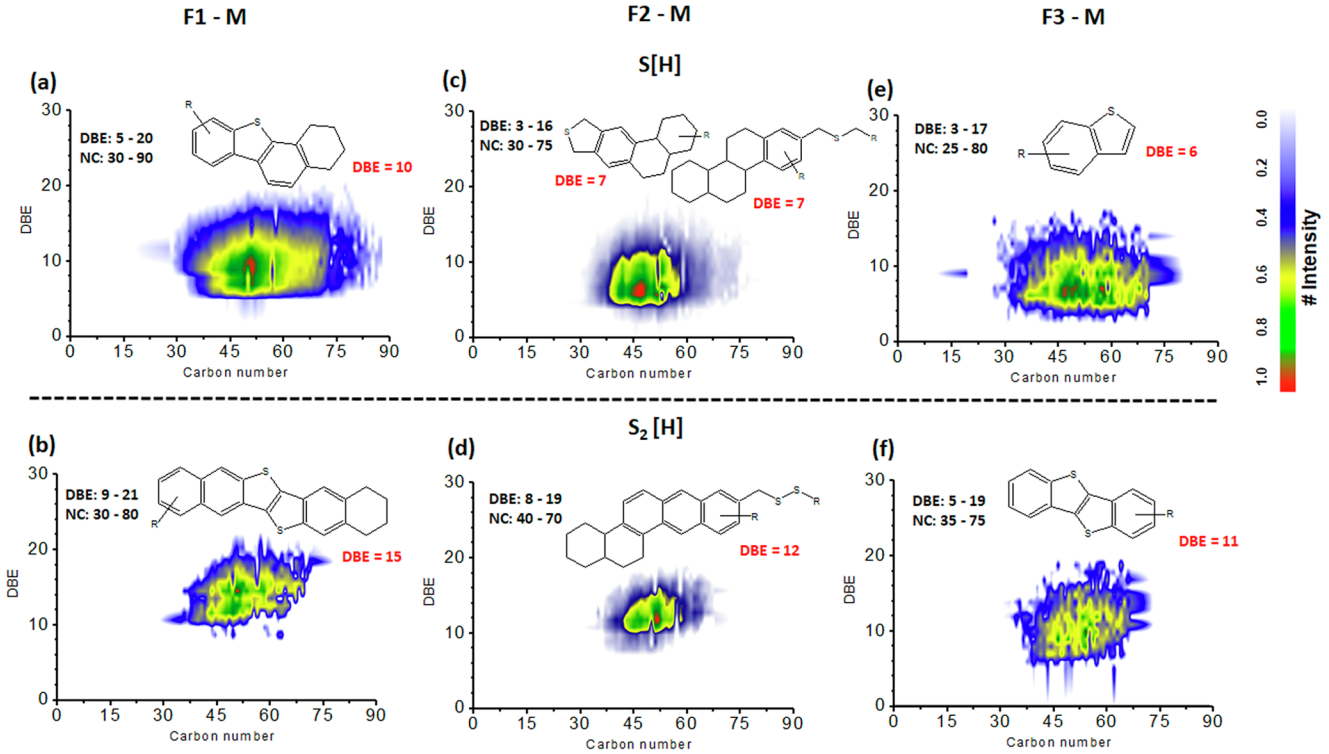

Fig. 8. DBE distribution as a function of the carbon number of S_1[H] (a–c) and S_2[H] (d–f) classes for the F1-M, F2-M, and F3-M fractions of AC 2.

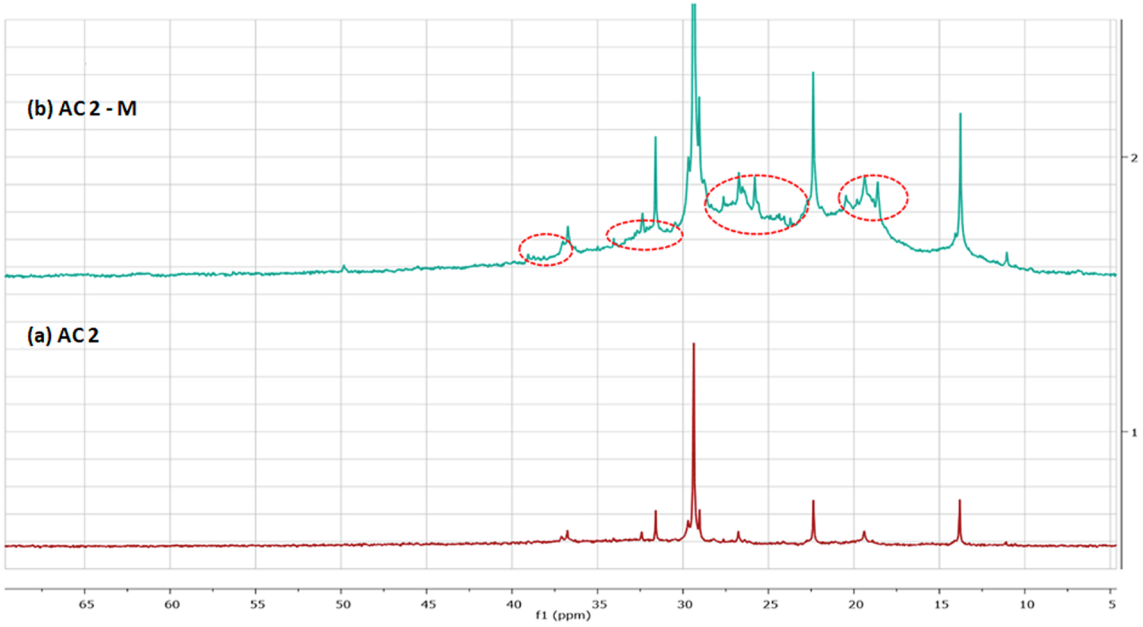

Fig. 9. ^{13}C NMR spectra of AC 2 sample (a) before and (b) after methylation reaction. The signals of methyl groups added to the sulfur atom are highlighted.

after methylation were analyzed to identify the types of sulfur compounds present in the sample. These values were compared with the δ values found in the literature for the ^{13}C methyls bound to sulfur in different types of sulfur compounds [38,39].

Comparing the ^{13}C NMR spectra before and after methylation (Fig. 9a, b), a clear difference is observed. In the methylated sample NMR spectrum, the emerging of several signals is noted (Fig. 9b, signals highlighted by a circle). These chemical shifts refer to the methyl group added to the sulfur in the methylation reaction [38,39]. It is essential to highlight that many signals were not attributed to any structure because they were not described in the literature. The chemical shifts detected are in the characteristic region of thiophenes structures (35.0, 34.06, 30.45, and 28.33 ppm), sulfides directly attached to aromatic rings (26.52, 25.14, and 21.87 ppm), sulfur heterocycles (25.80 ppm), and sulfide species in aliphatic chains or attached to carbon bonded to aromatic ring (22.27 and 21.87 ppm) [39]. ^{13}C NMR spectra also detect labeled compounds that can be attributed to methylation of other heteroatoms such as oxygen (see the small peak at ~50 ppm in Fig. 9b) and nitrogen.

To improve the assignment process of sulfur species by ^{13}C NMR technique, methylation reactions were performed on 10 model sulfur compounds to compare the ^{13}C chemical shift of the methyl group added to the different types of sulfur compounds, where their signals are easily detected as shown in Fig. 8S. Table 2 shows the sulfur compounds as tetrafluoroborate ($S^+BF_4^-$) salts and their ^{13}C chemical shifts values corresponding to bonding between the methyl group and the sulfur atom. Comparing the regions of the ^{13}C NMR spectra among the model sulfur compounds samples, Fig. 8S, with the AC 2 sample (Fig. 9) it is possible to prove that the signals detected in the last sample are consistent with characteristic signals of sulfur compounds. The thiophenic-type compounds (such as 3-methylbenzothiophene, 4,6-diethylbenzothiophene, naphtho [1,2-*b*: 5,6-*b*′] dithiophene, benzothiophene and dibenzothiophene) showed signals at 30.9, 32.0, 28.9–26.3, 30.6 and 33.6 ppm, respectively. Comparing these values with the chemical shifts that emerged for the AC 2-M sample, it is noted that these signals appeared in the region closer to the chemical shifts of the thiophene compounds, proving that they are consistent with thiophenes derivatives. Besides, the propanethiol, diphenyl sulfide, and tetrahydrothiophene compounds showed signals in 23.7, 27.1 and 24.5 ppm, respectively. These signals were also detected in the AC 2-M, evidencing the presence of less aromatic compounds, such as sulfides, mercaptans, and sulfur heterocycles species.

Table 2
^{13}C chemical shift for the methyl group added to S atom for several types of model sulfur compounds studied.

Model sulfur compound	^{13}C Chemical shift (ppm) of CH_3 group bonded to S
Propanethiol	23.7
2-Naphthalenethiol	14.6
3-Methylbenzothiophene	30.9
4,6-Diethylbenzothiophene	32.0
Diphenyl sulfide	27.1
Naphtho[1,2-*b*:5,6-*b*′]dithiophene	28.9, 27.2, 26.3, 23.4, 15.1, and 13.2
Diisopropyl sulfide	14.1
Tetrahydrothiophene	24.5
Benzothiophene	30.6
Dibenzothiophene	33.6

3.3. ESI(+) Q-Exactive Orbitrap MS

To evaluate the performance of organosulfur characterization between two high-resolution mass instruments (FT-ICR MS and Q-Exactive Orbitrap), ESI(+) Q-Exactive Orbitrap MS analyses were also performed for AC and maltene samples, before and after the methylation reaction, Figs. 10a–f, 9S and 10S. For the unmethylated samples, the amplitude of the signals ranged from *m/z* 200 to 700 (Fig. 10a–c), whereas after methylation, this range was *m/z* 200–800 (Fig. 10d, f), and *m/z* 200–1100 (Fig. 10e). Comparing the chemical profile of the maltene samples between the techniques of Orbitrap MS and ESI(+)FT-ICR MS (Fig. 3), the Q-Exactive Orbitrap MS was efficient in detecting compounds with lower M_w. Figs. 11, and 11S illustrate the DBE plot as a function of CN for S_1[H] and S_2[H] classes of ACs and maltenes, both methylated, respectively. DBE *vs.* CN graphs of the AC-M samples (except for AC 1) of the S_1[H] class obtained by the ESI(+)-FT-ICR MS analyses (Fig. 5c) and Orbitrap (Fig. 11b, c) were compared. A shift for lower DBEs distribution is observed, but these values were close to those detected by the FT-ICR MS. The DBE graphs obtained by FT-ICR MS (Fig. 5) were shifted to higher values of CN.

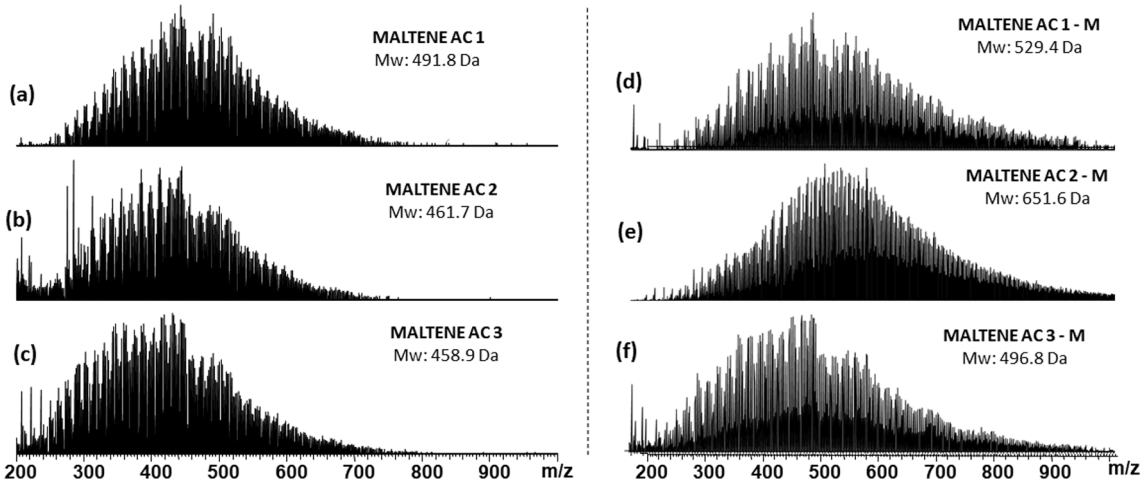

Fig. 10. ESI(+) Q-Exactive Orbitrap mass spectra of the maltenes (a–c) before and (d–f) after methylation.

3.4. Correlation between the organosulfur chemical profile and physical properties of asphalts

Fig. 12 shows the main proposed chemical structures detected in the S_1[H] and S_2[H] classes by ESI(+)FT-ICR MS (Figs. 8 and 7S) in the sulfur fractions of AC 1, AC 2, and AC 3 samples. Concerning the AC 1 sample, it is observed that it differs in function of aromaticity degree because the most abundant sulfur species detected in this sample were sulfur heterocycles in naphthenic rings. Therefore, the AC 1 sample presents a higher saturated character. On the other hand, in the AC 2 and AC 3 samples, the sulfur compounds are mainly detected as thiophene and aromatic sulfide compounds, which present a higher aromatic character. However, in the AC 2 sample, these species have higher aromaticity degree and M_w values than the AC 3 sample. Thus, in terms of aromaticity of the main sulfur compounds present, AC 2 sample has the most aromatic character and the AC 3, the lower character.

Some studies have shown that sulfur-containing species, with high aromaticity, are more stable to oxidation processes with species of lower aromaticity [11,41]. Thus, it is possible to infer that the AC 2 sample would be less susceptible to changes in the aging process because it has a higher concentration of sulfide compounds, which present higher aromaticity. Likewise, the AC 1 sample would be the most susceptible to oxidative processes because it has a higher concentration of saturated sulfur compounds, which have lower aromaticity, and are more reactive. Therefore, it suggests an order of stability in the aging process, based on the reactivity of the main sulfur compounds detected in the samples, which would be: AC 2 > AC 3 > AC 1.

Fig. 12S and Table 1 show a comparison of the physical properties such as “increase of the softening point” and “capillarity viscosity ratio,” which demonstrate the variation of the softening point and viscosity properties, respectively, after the RTFOT test. The RTFOT test

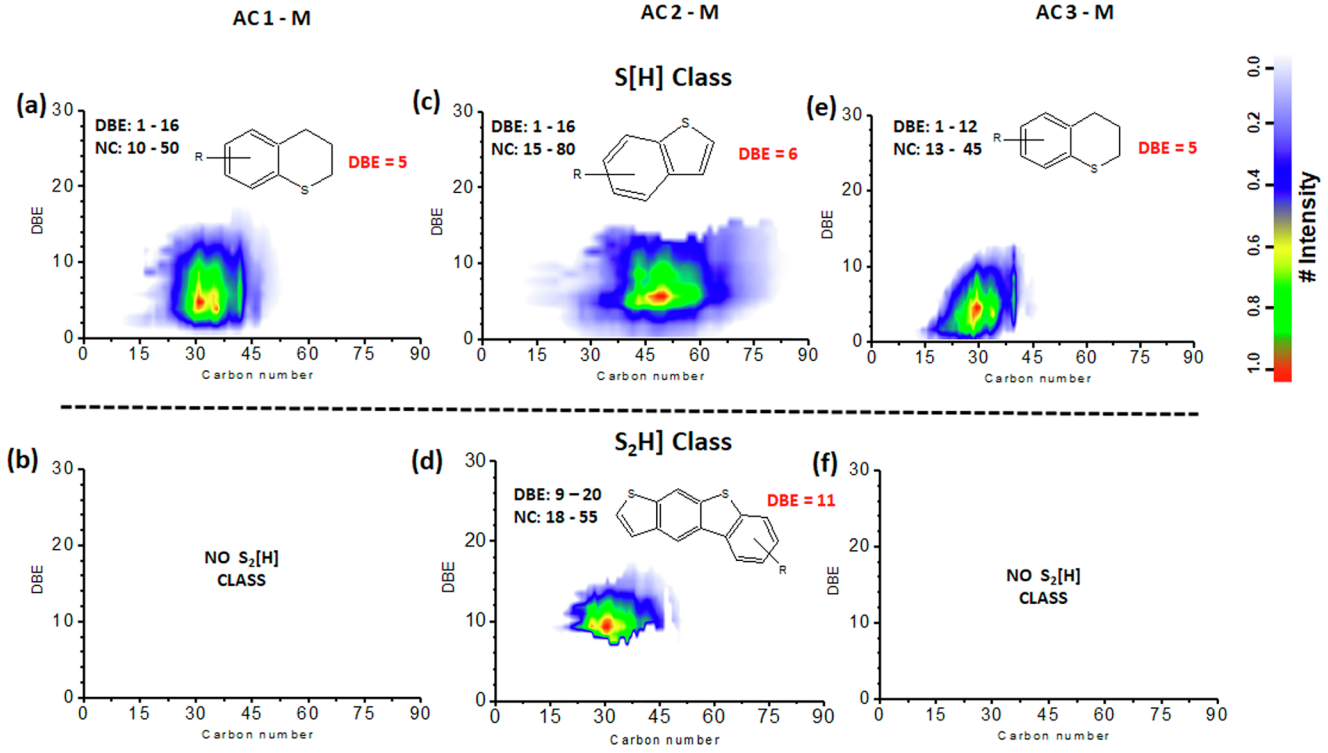

Fig. 11. DBE distribution as a function of carbon numbers of S_1[H] and S_2[H] classes of the methylated AC samples obtained by the ESI(+)Q-Exactive Orbitrap MS.

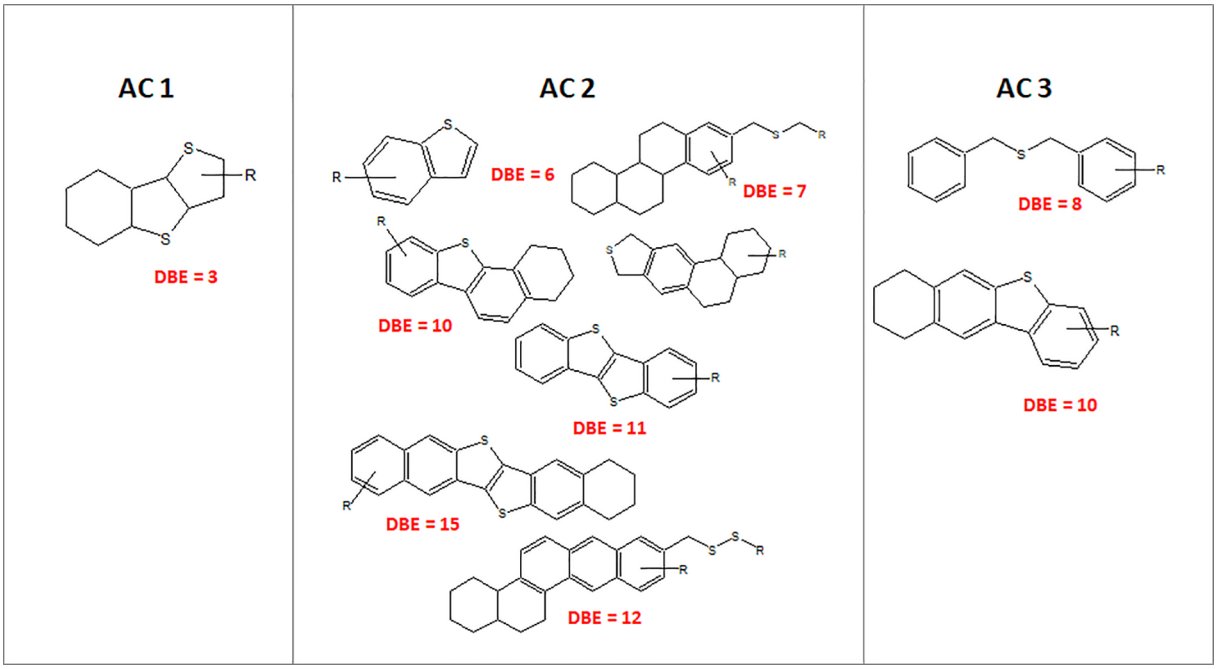

Fig. 12. Proposed structures for main organosulfur compounds detected from the $S_1[H]$ and $S_2[H]$ classes by ESI(+)FT-ICR MS in the sulfur fractions of AC 1, AC 2, and AC 3 samples.

simulates the short-term aging of asphalt during the hot mix, truck and silo storage, spray, and compaction processes, which take place during its application [4]. It is observed that the AC 1 sample was the one that suffered the most significant properties variation after the RTFOT test, thus demonstrating its higher susceptibility to aging. One of the factors that may have contributed is the presence of a higher reactive species concentration, i.e., saturated sulfur compounds, that participate directly in the oxidation reactions, generating a higher amount of polar products, which may interfere with the physical characteristics of AC.

On the other hand, the AC 2 sample had the lowest properties variation after RTFOT. This fact is probably due to the high concentration of aromatic sulfur compounds, which are less reactive and, therefore, will suffer less change during the oxidation process. Therefore, it is expected that they generate less polar compounds in asphalt aging processes. Hence, it is proved that the organosulfur chemical profiles directly affect the physicochemical properties of AC samples as well as their aging processes.

4. Conclusion

Despite the high complexity of the samples, this work showed that the methodology of organosulfur characterization of AC, using SPE and ESI(+)FT-ICR MS techniques are efficient methods that allow a higher amplitude in the detection of sulfur compounds. The use of SPE reduces the ion suppression effect and decreases the matrix complexity for the compounds of interest. These advantages contribute to the better efficiency of higher complexity organosulfur ionization, allowing a superior AC characterization. Moreover, ^{13}C NMR identified various types of sulfur compounds such as thiophene species, and aliphatic and aromatic sulfides, corroborating with the results obtained by ESI(+)FT-ICR MS. The comparison between the Orbitrap MS and ESI(+)FT-ICR MS techniques demonstrated that, for the samples under study, the Q-Exactive Orbitrap MS was efficient in the detection of compounds with lower M_w. In contrast, FT-ICR MS showed better efficiency in the ionization of molecules with higher values of CN. The organosulfur chemical profile was correlated to the "increase of the softening point" and "capillarity viscosity ratio" properties of AC samples. It was verified that the sample with higher aromatic character are less susceptible in the aging test, while the one with more saturated character presented more considerable variation in their physical properties after the aging test. Hence, it is proved that the chemical profile of organosulfur species directly affects the physicochemical properties of AC samples as well as their aging processes. In general, it was proved the high applicability of the ESI(+)FT-ICR MS technique combined with SPE in the organosulfur characterization present in ACs, contributing to better understanding the aging processes that occur in this matrix.

Acknowledgments

The authors thank CNPq, Fapes, and Petrobras for their financial support; and the Núcleo de Competências em Química do Petróleo (UFES), coordinated by Prof. Dr. Eustaquio V. R. Castro, for the FT-ICR MS analyses. "This study was financed in part by the Coordenação de Aperfeiçoamento De Pessoal De Nível Superior - Brasil (CAPES) – "Finance Code 1".

Appendix A. Supplementary data

Supplementary data to this article can be found online at https://doi.org/10.1016/j.fuel.2019.115923.

References

[1] Nascimento PC, Gobo LA, Bohrer D, Carvalho LM, Cravo MC, Leite LF. Determination of polycyclic aromatic hydrocarbons in fractions in asphalt mixtures using liquid chromatography coupled to mass spectrometry with atmospheric pressure chemical ionization. J Sep Sci 2015;38:2238–44.
[2] Yin Y, Chen H, Kuang D, Song L, Wang L. Effect of chemical composition of aggregate on interfacial adhesion property between aggregate and asphalt. Constr Build Mater 2017;146:231–7.
[3] Iqbal MH, Hussein HI, Al-Abdul Wahhab HI, Amin HB. Rheological investigation of the influence of acrilate polymers on the modification of asphalt. J Appl Polym Sci 2006;102:3446–56.
[4] Carvalho LM, Nascimento PC, Bohrer D, Claussen LE, Ferraz L, Grassmann C, et al. Distribution of total sulfur in acidic, basic and neutral fractions on Brazilian asphalt cements and its relationship to the aging process. Energy Fuel 2015;29:1431–7.
[5] Petersen JC, Hansberger PM, Robertson RE. Factors affecting the kinetics and mechanism of asphalt oxidation and the relative effects of oxidation products on age hardening. Am Chem Soc Fuel Chem Preprints 1996;41:1232–44.

[6] Michalica P, Kazatchokov IB, Stastna J, Zanzotto L. Relationship between chemical and rheological properties of two asphalts of different origins. Fuel 2008;87:3247–53.
[7] Silveira GD, Hoinacki CK, Goularte RB, Nascimento PC, Bohrer D, Cravo M, et al. A cleanup method using solid phase extraction for the determination of organosulfur compounds in petroleum asphalt cements. Fuel 2017;202:206–15.
[8] Carvalho LM, Grassmann CS, Nascimento PC, Bohrer D, Fröhlich AC, Hoinacki CK, et al. Distribution of sulfur compounds in Brazilian asphalt cements and its relationship to short-term and long-term aging processes. Constr Build Mater 2016;117:72–9.
[9] Sarret G, Connan J, Kasrai M, Eybert-Berard L, Bancroft M. Characterization of sulfur in asphaltenes by sulfur K- and L-edge XANES. J. Synchrotron Rad 1999;6:670–2.
[10] Wiltifong R, Mitra-Kirtley S, Muliins OC, Andrews B, Fujisawa G, Larsen JW. Sulfur speciation in different kerogens by xanes spectroscopy. Energy Fuel 2005;19(5):1971–6.
[11] Mill T. The role of hydroaromatics in oxidative aging in asphalt. Preprints of 212th ACS national meeting. 1996. p. 1245–9.
[12] Silveira GD, Faccin H, Claussen L, Goularte RB, Nascimento PC, Bohrer D, et al. A liquid chromatography–atmospheric pressure photoionizationtandem mass spectrometric method for the determination of organosulfur compounds in petroleum asphalt cements. J Chromatogr A 2016;1457:29–40.
[13] Han Y, Zhang Y, Xu C, Hsu CS. Molecular characterization of sulfur-containing compounds in petroleum. Fuel 2018;221:144–58.
[14] Li M, Wang TG, Simoneit BRT, Shi S, Zhang L, Yang F. Qualitative and quantitative analysis of dibenzothiophene, its methylated homologues, and benzonaphthothiophenes in crude oils, coal, and sediment extracts. J Chromatogr A 2012;1233:126–36.
[15] Mahé L, Dutriez T, Courtiade M, Thiébaut D, Dulot H, Bertoncini F. Global approach for the selection of high temperature comprehensive two-dimensional gas chromatography experimental conditions and quantitative analysis in regards to sulfur-containing compounds in heavy petroleum cuts. J Chromatogr A 2011;1218(3):534–44.
[16] Vasconcelos GA, Pereira RCL, Santos CF, Carvalho VV, Tose LV, Romão W, Vaz BG. Extraction and fractionation of basic nitrogen compounds in vacuum residue by solid-phase extraction and characterization by ultra-high resolution mass spectrometry. Int J Mass Spectrom 2017;418:67–72.
[17] Hegazi AH, Andersson JT. Limitations to GC-MS determination of sulfur-containing polycyclic aromatic compounds in geochemical, petroleum, and environmental investigations. Energy Fuels 2007;21:3375–84.
[18] Wang M, Zhu G, Ren L, Liu X, Zhao S, Shi Q. Separation and characterization of sulfur compounds in ultra-deep formation crude oils from Tarim Basin. Energy Fuels 2015;29:4842–9.
[19] Robson WJ, Sutton PA, McCormack P, Chilcott NP, Rowland SJ. Class type separation of the polar and apolar components of petroleum. Anal Chem 2017;89:2919–27.
[20] Hsu CS, Hendrickson CL, Rodgers RP, McKenna AM, Marshall AG. Petroleomics: advanced molecular probe for petroleum heavy ends, special feature: perspective. J Mass Spectrom 2011;46:337–43.
[21] Lobodin VV, Juyal P, McKenna AM, Rodgers RP, Marshall AG. Silver cationization for rapid speciation of sulfur-containing species in crude oils by positive electrospray ionization Fourier. Energy Fuels 2014;28:447–52.
[22] Liu P, Shi Q, Chung KH, Zhang Y, Pan N, Zhao S, et al. Molecular characterization of sulfur compounds in Venezuela crude oil and its SARA fractions by electrospray ionization Fourier transform ion cyclotron resonance mass spectrometry. Energy Fuels 2010;24(9):5089–96.
[23] Barros EV, Dias HP, Pinto FE, Gomes AO, Moura RR, Cunha Neto A, et al. Characterization of naphthenic acids in thermally degraded petroleum by ESI (−)-FT-ICR MS and 1H NMR after solid phase extraction (SPE) and liquid/liquid extraction. Energy Fuels 2018;23:2878–88.
[24] Pinto FE, Silva CFPM, Tose LV, Figueiredo MAG, Souza WC, Vaz BG, et al. Evaluation of adsorbent materials for the removal of nitrogen compounds in vacuum gas oil by ESI(±)FT-ICR MS. Energy Fuels 2017;31:3454–64.
[25] Terra LA, Filgueiras P, Pereira R, Gomes A, Vasconcelos GA, Tose LV, et al. Prediction of total acid number in distillation cuts of crude oil by ESI(−) FT-ICR MS coupled with chemometric tools. J Braz Chem Soc 2017;28:1822–9.
[26] Carvalho VV, Vasconcelos GA, Tose LV, Santos H, Cardoso FMR, Fleming F, et al. Revealing the chemical characterization of asphaltenes fractions produced by N-methylpyrrolidone using FTIR, molecular fluorescence, 1H NMR, and ESI(±)FT-ICR MS. Fuel 2017;210:514–26.
[27] Pinto FE, Barros EV, Tose LV, Souza LM, Terra LA, Poppi RJ, et al. Fractionation of asphaltenes in n-hexane and on adsorption onto $CaCO_3$ and characterization by ESI (+)FT-ICR MS: Part I. Fuel 2017;210:790–802.
[28] Romão W, Tose LV, Vaz BG, Sama SG, Lobinski R, Giusti P, et al. Petroleomics by direct analysis in real time-mass spectrometry. J Am Soc Mass Spectrom 2016;27:182–5.
[29] Purcell JM, Juyal P, Kim DG, Rodgers RP, Hendrickson CL, Marshall AG. Sulfur speciation in petroleum: atmospheric pressure photoionization or chemical derivatization and electrospray ionization Fourier transform ion cyclotron resonance mass spectrometry. Energy Fuels 2007;21(5):2869–74.
[30] Haapala M, Purcell JM, Saarela V, Franssila S, Rodgers RP, Hendrickson CL, et al. Microchip atmospheric pressure photoionization for analysis of petroleum by Fourier transform ion cyclotron resonance mass spectrometry. Anal Chem 2009;81(7):2799–803.
[31] Panda SK, Andersson JT, Schrader W. Characterization of supercomplex crude oil mixtures: what is really in there? Angew Chem 2009;48(10):1788–91.
[32] Shi Q, Pan N, Chung PLH, Zhao S, Zhang Y, Xu C. Characterization of sulfur compounds in oilsands bitumen by methylation followed by positive-ion electrospray ionization and fourier transform ion cyclotron resonance mass spectrometry. Energy Fuels 2010;24:3014–9.
[33] Ruddy BM, Hendrickson CL, Rodgers RP, Marshall AG. Positive ion electrospray ionization suppression in petroleum and complex mixtures. Energy Fuels 2018;32:2901–7.
[34] Wang X, Schrader W. Selective analysis of sulfur-containing species in a heavy crude oil by deuterium labeling reactions. Int J Mol Sci 2015;16:30133–43.
[35] Dalmaschio GP, Malacarne MM, Almeida VDL, Pereira TM, Gomes OG, Castro EVR, et al. Characterization of polar compounds in a true boiling point distillation system using electrospray ionization FT-ICR mass spectrometry. Fuel 2014;115:190–202.
[36] Müller H, Schrader W, Andersson JT. Characterization of high-molecular-weight sulfur-containing aromatics in vacuum residues using fourier transform ion cyclotron resonance mass spectrometry. Anal Chem 2005;77:2536–43.
[37] Panda SK, Schrader W, Al-Hajji A, Andersson JT. Distribution of polycyclic aromatic sulfur heterocycles in three Saudi Arabian crude oils as determined by fourier transform ion cyclotron resonance mass spectrometry. Energy Fuels 2007;21:1071–7.
[38] Green TK, Whitley P, Wu K, Lloyd WG, Zhuigan L. Structural characterization of sulfur compounds in petroleum by S-methylation and 13C NMR spectroscopy. Energy Fuels 1994;8:244–8.
[39] Joramillo JCP, Molina VD, Baldrich C. Semiquantitative analysis of thiophenic compounds in light cycle oil (LCO) using 13C NMR spectroscopy. Fuel 2004;83:337–42.
[40] Bennett B, Larter SR. Quantitative separation of aliphatic and aromatic hydrocarbons using silver ion-silica solid-phase extraction. Anal Chem 2000;72(5):1039–44.
[41] Lobodin VV, Robbins WK, Lu J, Rodgers RP. Separation and characterization of reactive and non reactive sulfur in petroleum and its fractions. Energy Fuels 2015;29:6177–86.
[42] De Conto JF, Santos MR, Carvalho AS, Campos KV, Freitas LS, Benvenutti EV, et al. Naphthenic acids recovery from petroleum using ionic silica based hybrid material as stationary phase in solid phase extraction (SPE) process. Adsorption 2014;20(8):917–23.
[43] Lunandes E, GREIBROKK T. Group separation of oil residues by supercritical fluid chromatography. J Chromatogr 1985;349:439–46.
[44] Method 384-76. Nitrogen in petroleum distillates and heavy oils by acid extraction or direct Kjeldahl procedure. West Consohocken, PA: UOP Inc; 1976.
[45] Method 269. Nitrogen bases in hydrocarbons by potentiometric titration. West Conshohocken, PA: UOP Inc; 1990.
[46] ASTM D664. Acid number of petroleum products by potentiometric titration. West Conshohocken, PA: ASTM International; 2011.
[47] ASTM D1552. Sulfur in petroleum products by high temperature combustion and infrared (IR) detection or thermal conductivity detection (TCD). West Conshohocken, PA: ASTM International; 2016.
[48] ASTM D5. Penetration of bituminous materials. West Conshohocken, PA: ASTM International; 2005.
[49] ASTM D36. Softening point of bitumen (ring-and-ball apparatus). West Conshohocken, PA: ASTM International; 2006.
[50] ASTM D2171. Viscosity of asphalts by vacuum capillary viscometer. West Conshohocken, PA: ASTM International; 2010.
[51] ASTM D2872. Effect of heat and air on a moving film of asphalt (rolling thin-film oven test). West Conshohocken, PA: ASTM International; 2012.
[52] ASTM D6560-00. Determination of aspaltenes (heptane insolubles) in crude petroleum and petroleum products. West Conshohocken, PA: ASTM International; 2000.
[53] Read J, Whiteoak D. The shell bitumen handbook. 5ª ed. Cambridge: Thomas Telford; 2003. p. 11–2.
[54] Liu P, Shi Q, Pan P, Zhang Y, Chung KH, Zhao S, et al. Distribution of sulfides and thiophenic compounds in VGO subtractions: characterized by positive-ion electrospray fourrier transform ion cyclotron resonance mass spectrometry. Energy Fuels 2011;25:3014–20.